

Deciphering the Positional Influence of the Hydroxyl Group in the Cinnamoyl Part of 3-Hydroxy Flavonoids for Structural Modification and Their Interaction with the Protonated and B Form of Calf Thymus DNA Using Spectroscopic and Molecular Modeling Studies

Ankur Bikash Pradhan,[†] Lucy Haque,[†] Sutanwi Bhuiya,[†] Aniruddha Ganguly,[‡] and Suman Das^{*†}

[†]Department of Chemistry, Jadavpur University, Raja S. C. Mullick Road, Jadavpur, Kolkata, West Bengal 700032, India

[‡]University of Calcutta, Senate House, 87/1, College Street, Kolkata, West Bengal 700073, India

S Supporting Information

ABSTRACT: Studies on the interaction of naturally occurring flavonoids with different polymorphic forms of nucleic acid are helpful for understanding the molecular aspects of binding mode and providing direction for the use and design of new efficient therapeutic agents. However, much less information is available on the interactions of these compounds with different polymorphic forms of DNA at the molecular level. In this report we investigated the interaction of two widely abundant dietary flavonoids quercetin (Q) and morin (M) with calf thymus (CT) DNA. Spectrophotometric, spectropolarimetric, viscosity measurement, and molecular docking simulation methods are used as tools to delineate the binding mode and probable location of the flavonoids and their effects on the stability and conformation of DNA. It is observed that in the presence of the protonated form of DNA the dual fluorescence of Q and M resulting from the excited-state intramolecular proton transfer (ESIPT) is modified significantly. Structural analysis showed Q and M binds weakly to the B form (groove binding) compared to the protonated form of CT DNA (electrostatic interaction). In both cases, Q binds strongly to both forms of DNA compared to M.

Structural Modification and Mode of DNA Binding of Flavonoids					
STRUCTURAL MODIFICATION			MODE OF DNA BINDING		
pH	Flavonoid	Emission	Protonated DNA	Flavonoid	B-DNA
		Free Normal Tautomer			
		DNA Bound Normal Tautomer			
3.4	Q	✓	✗	✓	✓
	M	✓	✗	✓	✓
7.0	Q	✓	✓	✓	✓
	M	✗	✓	✗	✓

External Stacking

Minor Groove Binding

Major Groove Binding

INTRODUCTION

Protonation-induced structures of nucleic acids play a crucial role as pH is a very important factor in biological processes. It is now well established that the protonation results in significant changes in DNA conformation, which is dependent on the base composition of the nucleic acids and the ionic strength of the medium.^{1,2} It is suggested that protonation causes the formation of a unique left-handed conformation of DNA with Hoogsteen base pairing, and it is stable at low temperature and low ionic strength.³ The stability of the protonated conformation is significantly different from the right-handed B form and left-handed Z form. This structural model has been confirmed from Raman and FTIR studies.⁴ It has been shown that cytosines followed by guanines are the primary protonation sites in DNA. Thus, protonation causes more changes on GC-rich DNAs than AT-rich DNAs. Natural DNAs containing both GC and AT base pairs undergo protonation-induced structural changes irrespective of base composition. In the case of AT base pairing the number of hydrogen bonds remains the same for both Watson–Crick and Hoogsteen base pairing. However, in the case of GC base pairing under low pH condition the number of hydrogen bonds decreases to two from three, which is observed in Watson–Crick base pairing under physiological pH (Scheme 1).

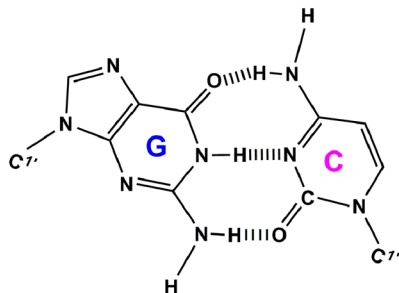
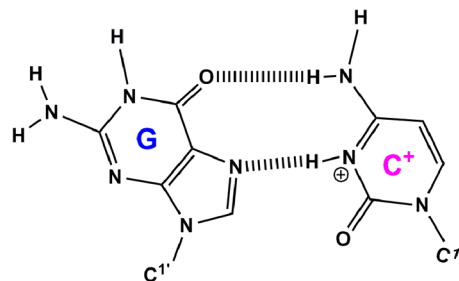
Flavonoids are naturally occurring polyphenolic compounds that are found in higher plants. They are low molecular weight organic compounds and categorized into flavonols, flavones, isoflavones, flavanones, anthocyanidins, catechins, and chalcones according to chemical structure. The flavonoids have gained substantial attention because of their prospective beneficial effects on human health. The basic structure is usually characterized by two aromatic rings (ring A and ring B). These rings are joined by three carbon atoms that link the γ -pyrone ring (ring C), forming a C6–C3–C6 skeleton where polar groups, usually hydroxyl or methoxy, appear at various positions. The efficiency of flavonoids as an antioxidant agent greatly depends on their chemical structures. Three structural features are the most important as observed by Jurasekova and her groups:⁵ (i) the catechol moiety in the B ring, which is a radical target site; (ii) the C2=C3 bond in conjugation with a 4-keto function in the γ -pyrone ring, which is responsible for electron delocalization from the B ring; and (iii) the presence of both 3- and 5-hydroxyl groups for radical scavenging. Further, the catechol moiety as well as the 4-keto and

Received: March 24, 2015

Revised: May 14, 2015

Published: May 15, 2015

Scheme 1. G-C Base Pairing of DNA of Watson–Crick and Hoogsteen Strands

Watson–Crick base pairing**Hoogsteen base pairing**

additional 3- or 5-hydroxyl groups play an important role in chelating metal ions.⁶ Flavonoids exert their functions usually by modifying the conformation of the nucleic acids. Thus, it is necessary to monitor the interaction between these flavonoid analogs and polymorphic forms of nucleic acids to understand the mechanism of drug action at molecular level.

Quercetin ($C_{15}H_{10}O_7$) (3,3',4',5,7-pentahydroxyflavone, Q, Figure 1A) and morin (3,5,7,2',4'-pentahydroxyflavone, M,

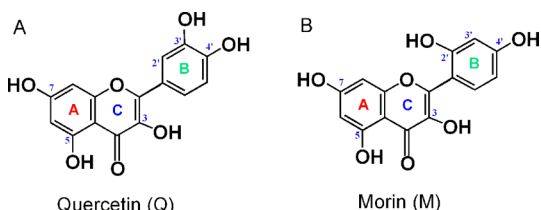
**Figure 1.** Chemical structure of quercetin (Q) and morin (M).

Figure 1B) are the most common naturally occurring flavonoids. These are the most well-characterized group of polyphenolic compounds. The basic difference in the structures of these flavonoids is the presence of a catechol moiety in Q. Both Q and M belong to the family of 3-hydroxyflavone (3-HF). One of the notable structural features of the 3-HF is their ability to show pH-dependent dual-fluorescence behavior in the excited state.

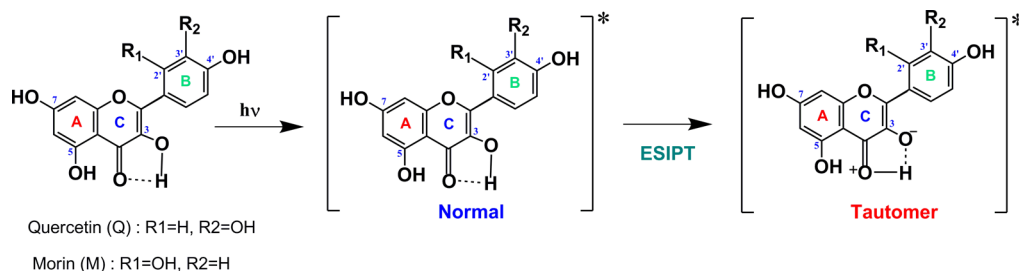
The presence of a 3-hydroxyl group in the γ -pyrone ring is responsible for such dual-fluorescence behavior. The dual fluorescence of flavonoid was first reported by Frolov et al.⁷ However, the reason for this behavior was explained by Sengupta and Kasha.⁸ It is now widely accepted that the normal molecule in the excited state tautomerizes through intramolecular proton transfer across the internal hydrogen bond of

the 3-hydroxyl group to the carbonyl oxygen in the γ -pyrone ring (Scheme 2).

Binding of small molecule with different polymorphic forms of nucleic acids has been an important area of investigation in the last few decades. Small molecules interact differentially with different polymorphic forms of nucleic acids. Thus, a better understanding of the molecular aspects of the interaction provides the scope for successful design of compounds for therapeutic purposes. The interactions of small molecules like flavonoids with double-stranded CT DNA have biological relevance.

Protonation of nucleic acid has gained considerable significance, and the biological relevance of low-pH-induced nucleic acid structures has been demonstrated.² With a large variety of accessible conformations it is expected that the protonated form of DNA will be found to have more biological importance. Keeping in view the biological relevance of the protonated structure of DNA and naturally occurring flavonoids we first systematically studied the photophysical properties of two flavonoids, Q and M, and then we focused on their interaction with different polymorphic forms of CT DNA.

The possible binding modes between these two molecules and DNA were determined by viscometric measurements and molecular modeling study. Such studies yield information about the binding mechanism and the conformation of flavonoid–DNA complex. Even though much is reported about the biological activities of flavonoids, little detail has been delineated about their interactions with individual DNA and RNA. Therefore, it encourages us to investigate the interaction of these flavonoids with polymorphic forms of DNA at the molecular level. Detailed studies on these flavonoids will explore their biological roles. This work provides valuable information about the photophysical properties and binding mechanism of Q and M with the protonated form of DNA and

Scheme 2. Schematic Diagrams Depicting the Ground and Excited (denoted by an asterisk (*)) States of Normal and Tautomer Forms of the Flavonoid

should be helpful in designing new and effective therapeutic drugs in targeting specific DNAs at low pH.

MATERIALS AND EXPERIMENTAL METHODS

Nucleic Acid, Buffer, and Reagents. CT DNA, Q, and M were obtained from Sigma Chemical Co., St. Louis, MO, USA. They were used without any further purification. The concentration of CT DNA was determined by UV measurements using a molar extinction coefficient of $6600 \text{ M}^{-1} \text{ cm}^{-1}$ at 260 nm in terms of bases.⁹ Solutions of Q and M were prepared freshly each day. The concentrations of Q and M were calculated using molar extinction coefficients of $14920 \text{ M}^{-1} \text{ cm}^{-1}$ at 375 nm and $14945 \text{ M}^{-1} \text{ cm}^{-1}$ at 373 nm, respectively. All stock solutions were prepared in 10 mM citrate–phosphate (CP, pH 7.0) buffer containing 10 mM Na_2HPO_4 . Distilled deionized Millipore water was used throughout the whole experiment.

Buffers. Buffer solutions of different pH were prepared according to Gomori¹⁰ and are as follows.

- (1) Formation of the protonated DNA and interaction studies of flavonoids with this DNA conformation were carried out in citrate–phosphate (CP) buffer of pH 3.4 having a constant $[\text{Na}^+]$ of 10 mM, designated as buffer 1.
- (2) Citrate–phosphate (CP) buffer of pH 7.0 having a constant $[\text{Na}^+]$ of 10 mM designated as buffer 2. Nucleic acid stock solutions were prepared in buffer 2. Studies of the interaction of flavonoids with the B form of DNA were carried out in this buffer. The buffer solutions were filtered through $0.45 \mu\text{m}$ Millipore filters to avoid particulate matter.

Spectrophotometric Measurements. *UV–Vis Spectroscopy.* UV–vis absorbance studies were carried out on a Shimadzu model UV-1800 spectrophotometer (Shimadzu Corp., Japan). Matched quartz cells of 1 cm path length were used in this study. Respective buffer solutions were used as the reference. During optical titration of the flavonoids an equal amount of DNA was added to both the sample and the reference cells. The temperature of the sample and reference cells was controlled by the Peltier effect employing a thermoprogrammer attached to the instrument. In the spectrophotometric titrations to a fixed concentration of flavonoid, the concentration of DNA was varied and the change in the absorption at λ_{max} of the flavonoid was noted at each P/D [DNA/flavonoid molar ratio] until saturation was achieved.

Spectrofluorimetric Studies. *Fluorescence Spectral Analysis.* Steady-state fluorescence measurements were carried out on a Shimadzu RF-S301PC spectrofluorimeter (Shimadzu Corp., Kyoto, Japan). This was attached to a sensitive temperature controller. Measurements were made in a fluorescence free quartz cell of 1 cm path length. To a fixed concentration of flavonoid small aliquots of DNA solution were added under constant stirring condition. All measurements were performed keeping both the excitation and the emission slit at 5 nm.

Determination of Binding Stoichiometry. Job's continuation method¹¹ was used to evaluate the binding stoichiometry of flavonoids with CT DNA using fluorescence spectroscopy. At a fixed temperature the fluorescence intensity (at corresponding λ_{max}) was noted for the solutions where the concentrations of DNA and flavonoid were varied keeping the

sum of their concentrations fixed at $10 \mu\text{M}$. The relative difference of fluorescence intensity of flavonoids was plotted against the mole fraction of flavonoid. The mole fraction of the flavonoid in complex was obtained from the inflection point of the plot. The stoichiometry was obtained in terms of DNA:Flavonoid $[(1 - \chi_{\text{Flavonoid}})/\chi_{\text{Flavonoid}}]$, where $\chi_{\text{Flavonoid}}$ denotes the mole fraction of flavonoid.

Determination of Fluorescence Polarization Anisotropy. Fluorescence anisotropy (r) measurements were carried out as described by Larsson et al.¹² using

$$r = \frac{(I_{VV} - GI_{VH})}{(I_{VV} + 2GI_{VH})} \quad (1)$$

where G is the ratio I_{HV}/I_{HH} used for instrumental correction. I_{VV} , I_{VH} , I_{HV} , and I_{HH} represent the fluorescence signal for excitation and emission with the polarizer set at $(0^\circ, 0^\circ)$, $(0^\circ, 90^\circ)$, $(90^\circ, 0^\circ)$, and $(90^\circ, 90^\circ)$, respectively. For the time-resolved fluorescence anisotropy decay measurements, the polarized fluorescence decays for the parallel I_{VV} and perpendicular I_{VH} emission polarizations with respect to the vertical excitation polarization were first collected at the emission maxima of the flavonoid. The anisotropy decay function $r(t)$ was constructed using eq 1.

Fluorescence Lifetime Measurements. Time-correlated single-photon counting (TCSPC) measurements were carried out for the fluorescence decay of Q and M in the absence and presence of CT DNA in buffer 1 for protonated DNA at 10°C and in buffer 2 for the B form DNA and 25°C . Here the photoexcitation was made at 440 nm using a picosecond diode laser (IBH Nanoled-07) in an IBH fluorocube apparatus. The fluorescence decay data were collected on a Hamamatsu MCP photomultiplier (R3809) and analyzed by IBH DAS6 software using the equation

$$F(t) = \sum_i \alpha_i e^{-\frac{t}{\tau}} \quad (2)$$

where α_i is the i th pre-exponential factor and τ is the decay time. The decay time is the lifetime of the excited species.

Spectropolarimetric Measurements. *Circular Dichroism (CD) Titration.* CD measurements were performed on a JASCO J815 spectropolarimeter (Jasco International Co.). The instrument was attached with a highly sensitive temperature controller and a thermal programmer (model PFD-425L/15). A scan speed of 100 nm/min was used to record the CD spectra in the wavelength range of $200\text{--}450 \text{ nm}$. The CD spectra were expressed in terms of molar ellipticity ($[\theta]$, in units of $\text{deg cm}^2 \text{ dmol}^{-1}$), and molar ellipticity is based on DNA concentration. Measurements were done at 10 and 25°C for the protonated and B form of CT DNA, respectively.

Viscometric Study. A Cannon–Manning semimicrodilution viscometer type 75 (Cannon Instruments Co., State College, PA) was used for viscometric measurements. The viscometer was submerged vertically in a water bath maintained at $10 \pm 0.5^\circ\text{C}$ for the protonated form and at $25 \pm 0.5^\circ\text{C}$ for the B form of CT DNA. A $700 \mu\text{L}$ amount of $450 \mu\text{M}$ DNA solution was taken in the viscometer. Then aliquots of stock flavonoid solution were directly added into the viscometer to notice the change of viscosity with increasing D/P values. Flow times of the solutions were measured in triplicate with an accuracy of $\pm 0.01 \text{ s}$. The relative specific viscosity was evaluated using the equation

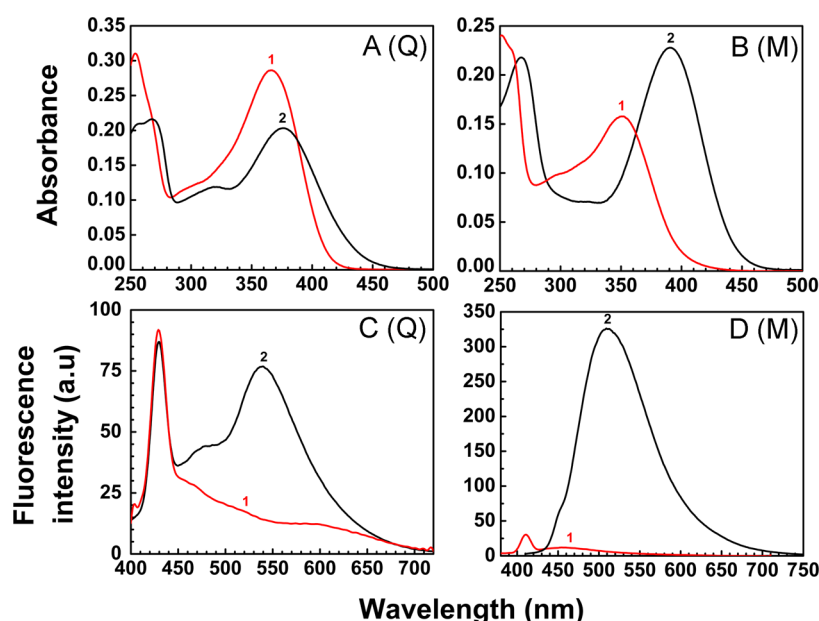


Figure 2. Representative UV spectra of 8.27 μM Q (A) and 7.29 μM M (B) and fluorescence emission spectra of 8.27 μM Q (C) and 7.29 μM M (D) in buffer 1 (curve 1) and buffer 2 (curve 2) at 10 and 25 $^{\circ}\text{C}$ respectively.

$$\frac{\eta'_{\text{sp}}}{\eta_{\text{sp}}} = \frac{[t_{\text{complex}} - t_0]}{[t_{\text{control}} - t_0]} \quad (3)$$

where η'_{sp} and η_{sp} are the specific viscosity of DNA in the presence and absence of flavonoid, t_{complex} and t_{control} are the time of flow of DNA–flavonoid complex and control solution, and t_0 is the same for buffer solution as described previously.¹³

Helix Melting Experiments. A helix melting study was performed using the same spectrophotometer equipped with the Peltier-controlled TMSPC-8 model accessory (Shimadzu Corp., Japan). Absorbance at different temperatures in the range 10–90 $^{\circ}\text{C}$ at 260 nm was noted for free DNA and DNA–flavonoid complexes. Melting profiles of all duplexes displayed single, cooperative transitions. The melting temperature T_m , the midpoint temperature of transition of the DNA denaturation process, can be estimated from the melting curves.

THEORETICAL METHODS

Density Functional Theory (DFT) Study. DFT is a useful tool for modeling electronic structure, electronic transition, UV spectrum, etc., for different molecules.^{14–16} DFT calculations were adopted to model the electronic structure and transitions of both the flavonoids Q and M. The Gaussian 09W program was used by considering the most probable structure. The B3LYP function has been adopted along with a 6-31G basis set for H, C, and O atoms. The energy for different sets of highest occupied molecular orbital (HOMO) and lowest unoccupied molecular orbital (LUMO) for the normal and photoproduct tautomer has been obtained from the DFT study. Using these data, we can get an idea about the dual-fluorescence behavior of the flavonoids in different pH of buffer solutions.

Molecular Modeling: Docking Study. The native structures of DNA were collected from the RSC Protein Data Bank having PDB ID 225D and BDL001 for the protonated and B form of DNA, respectively. Docking simulation studies were carried out with the AutoDock 4.2 software. This software uses the Lamarckian Genetic Algorithm (LGA) method. Gaussian 09W and Auto Dock 4.2 software packages were

used to create the required file of the flavonoid for the docking of the flavonoid with DNA. The structures of Q and M were first optimized at the DFT//B3LYP/6-31G level of theory using the Gaussian 09W program. The resultant geometries were read by using Gauss view 5 software in a compatible file format. From this, the required file was created using AutoDock 4.2. The grid box was set to 110, 110, and 110 Å along the X, Y, and Z axes with a 0.413 Å grid spacing. The Auto Docking parameters used were as follows: GA population size = 150; maximum number of energy evaluations = 225 000; GA cross-over mode = two points. The lowest energy conformation was taken for each simulation. Further analysis was done with the resultant minimum energy conformation. For better visualization of the docked conformations the PyMOL and Mercury 3.3 software packages were used.

RESULTS AND DISCUSSION

UV and CD Spectral Characteristics of Protonated and B Form of CT DNA. B form to protonated form of DNA conformational transition was initiated by slow addition of stock CT DNA solution to buffer 1 at 10.0 ± 0.5 $^{\circ}\text{C}$ under stirring. This structural transition was very fast and found to be completed in about 1 s.¹⁷ An equilibrium time of 5 min was allowed before measurements were carried out. In Figure S1A, Supporting Information, the characteristic UV spectra of the protonated (curve 1) and B (curve 2) forms of CT DNA are presented. A hypochromic effect in the 260 nm absorption band was observed in low pH. Thermal melting profiles of the protonated and B form of CT DNA are shown in the inset of Figure S1A, Supporting Information. Both forms of DNA exhibited sharp and cooperative melting transitions. The thermal melting temperature (T_m) value of the protonated form was remarkably less compared to the B form counterparts. T_m of the protonated form and B form of CT DNA were found to be 22 and 67 $^{\circ}\text{C}$, respectively. The marked difference in T_m between the protonated and the B form can be explained on the basis of the number of hydrogen bonds. Under low-pH condition the number of hydrogen bonds decreases to two

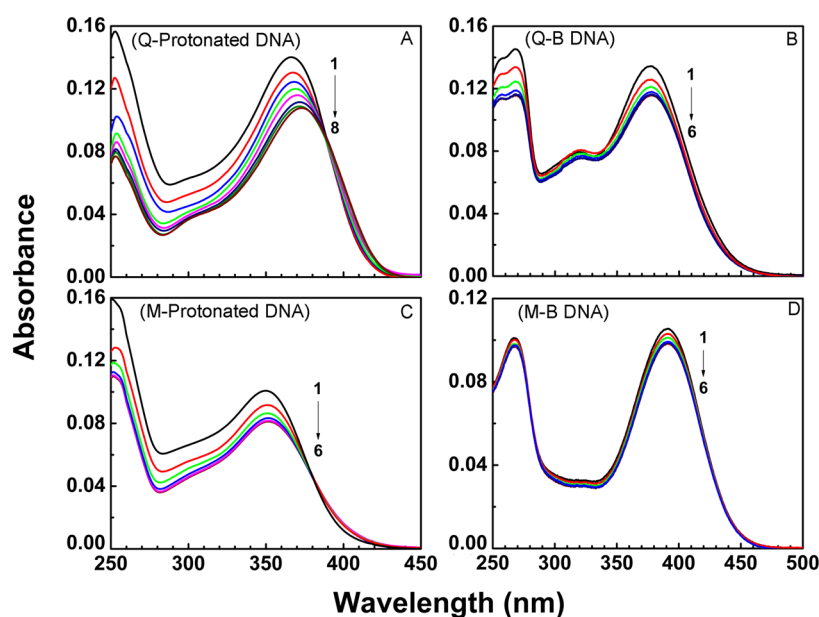


Figure 3. Absorption spectra of Q and M in the presence of CT DNA: (A) Spectra 1–8 denote the absorption spectrum of Q (5.15 μM) treated with 0, 8.29, 16.58, 24.88, 33.17, 41.46, 58.05, and 74.59 μM CT DNA in buffer 1 at 10 $^{\circ}\text{C}$; (B) Spectra 1–6 denote the absorption spectrum of Q (5.15 μM) treated with 0, 13.24, 24.49, 48.99, 63.48, and 112.47 μM CT DNA in buffer 2 at 25 $^{\circ}\text{C}$; (C) Spectra 1–6 denote the absorption spectrum of M (4.89 μM) treated with 0, 8.29, 24.88, 41.46, 74.59, and 107.17 μM CT DNA in 10 mM CP buffer of pH 3.4 at 10 $^{\circ}\text{C}$; (D) Spectra 1–6 denote the absorption spectrum of M (4.89 μM) treated with 0, 24.49, 48.99, 73.48, and 122.47 μM CT DNA in 10 mM CP buffer of pH 7.0 at 25 $^{\circ}\text{C}$.

from three in the case of GC base pairing. Therefore, under low-pH condition the thermal stability of protonated DNA decreases due to a decrease in the number of hydrogen bonds. Such decrease in T_m has been reported to be more pronounced in the case of DNA having a greater proportion of GC content.¹⁸ A sharp cooperative melting transition in the protonated form of CT DNA clearly reveals the duplex nature even at pH 3.4.^{9,17} CD spectra of the protonated (curve 1) and B (curve 2) form of CT DNA are shown in Figure S1B, Supporting Information. The CD spectrum of B-form DNA was characterized by a negative band at 245 nm and a positive CD band around 275 nm. At pH 3.4, the 275 nm band exhibited hypochromic and bathochromic shifts and the negative band ellipticity also decreased. In case of the protonated form, two positive bands around 255 and 290 nm appeared.

UV Absorption Spectra of Flavonoids at Different pH.

Two main absorption bands are observed in the UV spectra of flavonoids: (i) band I (300–450 nm), the absorption of the cinnamoyl part (B + C), and (ii) band II (250–285 nm), the conjugated system of ring A and ring C (γ -pyrone ring) in the molecule.^{19,20} Characteristic UV absorption spectra of Q and M in buffer 1 and buffer 2 are shown in Figure 2A and 2B. Recently, Z. Jurasekova and her group reported the pH-dependent structural changes of a group of flavonoids,⁵ and they concluded that the chemical modification is very significant for those flavonoids which possess (i) the C3–OH group in the γ -pyrone ring, (ii) the catechol moiety in the B ring, and (iii) the C2=C3 bond in the γ -pyrone ring. Here the chemical modifications are thought to be major for Q since it possesses all three features, and for M, which does not possess any catechol moiety, the modification is dominated by deprotonation of the phenolic –OH group at high pH condition. Deprotonation of the phenolic –OH group in the flavonoid molecule leads to the formation of a negative

oxygenic ion. This causes a significant bathochromic shift of the UV absorption bands due to the extended conjugation.^{19–21} For Q, the maximum UV absorption wavelength (λ_{max}) of band I at pH 3.4 was situated at 366 nm and it was red shifted to 376 nm when the pH of the buffer solution changed to 7.0 (Figure 2A). A similar result was also observed by Jurasekova et al.⁵ However, M shows a large shift of λ_{max} (from 350 to 390 nm) when the pH of the solution changes from 3.4 to 7.0. The reason for this significant red shift of M can be explained on the basis of its acidity. The $\text{p}K_{\text{a}1}$ and $\text{p}K_{\text{a}2}$ for M are 3.46 and 8.10, respectively, and the $\text{p}K_{\text{a}1}$ is significantly lower than that of Q ($\text{p}K_{\text{a}1} = 6.74$).²² Both flavonoids have almost the same structure except the ring B where the –OH groups are situated at different positions. The marked differences in the $\text{p}K_{\text{a}1}$ values may be attributed to this part of the molecules. It has been shown that the 4'–OH group in the B ring of M dissociates at neutral pH.²⁰ The generated phenoxide ion becomes stabilized through extended conjugation with ring C. For this reason, the $\text{p}K_{\text{a}1}$ value of M is very low and there is a large bathochromic shift of absorption maximum. However, in the case of Q, it seems that dissociation of the 3'–OH group in ring B occurs which cannot form a conjugate system with the γ -pyrone ring, and as a result less stabilization of the conjugate base is noted. Thus, the $\text{p}K_{\text{a}1}$ value of Q is higher compared to M.

The dissociation of the OH group at the 4' position on the cinnamoyl part (B + C) of the M molecule was indicated from the significant red shift of band I as shown in Figure 2B. From above results it can be concluded that the –OH group on the cinnamoyl part of the M molecule would be dissociated nearly completely in physiological condition (pH 7.0) due to its high acidity, and M mainly exists as an anionic species.

Emission Characteristics of Flavonoids at Different pH. The fluorescence emission spectra of Q and M in buffers 1 and 2 are presented in Figure 2C and 2D, respectively. The emission spectrum of flavonoid was monitored in the 370–750

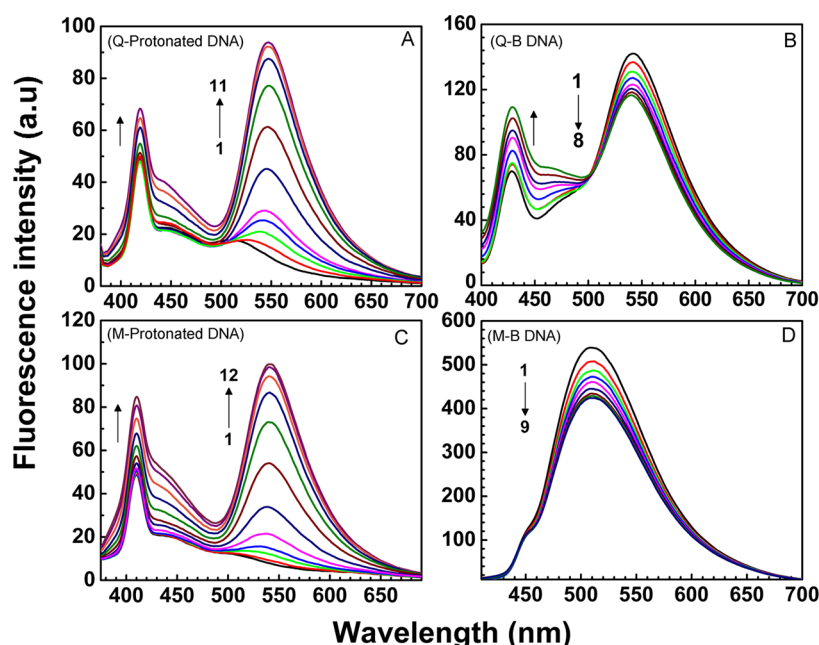


Figure 4. Fluorescence spectra of Q and M in the presence of CT DNA: (A) Spectra 1–11 denote the fluorescence spectrum of Q ($5.15 \mu\text{M}$) treated with 0, 0.59, 1.18, 2.36, 4.73, 9.46, 14.19, 33.11, 52.03, 75.68, and $99.33 \mu\text{M}$ protonated form of CT DNA in buffer 1 at 10°C ; (B) Spectra 1–8 denote the fluorescence spectra of Q ($5.15 \mu\text{M}$) treated with 0, 4.73, 9.46, 14.19, 23.65, 37.84, 56.76, and $80.41 \mu\text{M}$ B form of CT DNA in buffer 2 at 25°C ; (C) Spectra 1–12 denote the fluorescence spectrum of M ($4.89 \mu\text{M}$) treated with 0, 1.18, 2.36, 4.73, 9.46, 14.19, 33.11, 52.03, 75.68, 99.33, 122.98, and $151.36 \mu\text{M}$ protonated form of CT DNA in buffer 1 at 10°C ; (D) Spectra 1–9 denote the fluorescence spectrum of M ($4.89 \mu\text{M}$) treated with 0, 4.73, 9.46, 14.19, 23.65, 37.84, 56.76, 80.41, and $108.79 \mu\text{M}$ B form of CT DNA in buffer 2 at 25°C .

nm wavelength range. Photoexcitation of Q at 377 nm shows dual emission in buffer 2: one band maximum at ~ 420 nm corresponding to the normal and the other band at ~ 539 nm corresponding to the photoproduct tautomer (Figure 2C). However, no emission corresponds to the photoproduct isomer observed in buffer 1. Since the γ -pyrone ring (ring C) is responsible for the production of the tautomer there must be some mechanism that occurs in this ring, and we are concerned only about this part. In acidic condition there are three sites in ring C where protonation can occur. The phenolic OH group is itself acidic, and thus, protonation of this group can be ruled out. Protonation on the O-1 atom of the ring leads to dearomatization. Therefore, the only possible site for protonation is the carbonyl oxygen. For the carbonyl oxygen protonation occurs at low pH of the medium. Thus, due to protonation on the carbonyl oxygen the tautomerization could not occur (Scheme 2), and as a result, no photoproduct tautomer was obtained in the excited state. However, in the case of M, in buffer 1 no emission corresponding to the photoproduct isomer was observed, which was also due to the same reason as in the case of Q, but in buffer 2 photoexcitation of Q at 390 nm shows the emission spectrum with only one maximum at ~ 510 nm. Though a hump (may be due to the normal isomer) around ~ 450 nm is observed, it is overpowered by the strong emission peak corresponding to the photoproduct tautomer. The 3-HF group of flavonoids shows dual fluorescence with band maxima around 410–430 and 510–530 nm, corresponding to the normal and the photoproduct tautomer, respectively.^{23,24} Thus, the emission maximum of M in pH 7.0 is due to the emission of photoproduct tautomer only (Figure 2D), which is in contrast compared to the emission spectrum of Q. As said earlier, in buffer 2, M mainly exists as an anionic species due to complete dissociation of the $-\text{OH}$ group on the cinnamoyl part of the M molecule. Thus, in

this buffer M mainly exists as the tautomer, and it is also reflected from the emission spectra of M in buffer 2.

Absorption Spectral Study. Flavonoid-Protonated DNA Interaction. The addition of the protonated form of DNA shows a greater hypochromic effect in the absorption spectra of Q and M compared to the B form counterpart. However, the extent of hypochromicity is more in the case of Q (Figure 3A) compared to that of M (Figure 3C). In addition, a significant bathochromic shift (~ 6 nm) of Q is observed in the presence of protonated DNA, whereas an insignificant change is noted in the case of M. In general, if a small molecule interacts with nucleic acid, changes in absorbance (hypochromism) and in the bathochromic shift should occur. This phenomenon indicates a strong interaction between the aromatic chromophore and the base pairs of nucleic acids. Such spectral changes may be explained as follows:^{25,26} The coupling of the empty π^* orbital of the flavonoid with the π^* orbital of the DNA base pairs results the decrease of the $\pi - \pi^*$ transition energy, and consequently, there is a bathochromic shift of the absorption of the flavonoid. At the same time, the empty π^* orbital of the flavonoid is partially filled with electrons to reduce the transition probability, which leads to hypochromism. In both cases an isosbestic point is observed at ~ 389 nm for Q and at ~ 380 nm for M, which clearly establishes the equilibrium between the complex and the free flavonoid molecules.

Flavonoid B Form DNA Interaction. The effect of addition of B-form DNA on the UV–vis absorption of Q and M was examined in buffer 2. The absorption spectra of flavonoids showed strong absorbance at ~ 390 (band I) and ~ 265 nm (band II). Figure 3B and 3D shows the effect of increasing concentration of the B form of CT DNA on the absorption spectrum of Q and M, respectively. The addition of the B form of CT DNA shows a little hypochromic effect in the UV–vis spectra of Q and M without any significant shift of λ_{max} .

Table 1. Binding Parameters for the Association of Q and M with Protonated and B Form of CT DNA in Respective Buffers^a

dye	methods	polymer	$K_a \times 10^{-4} \text{ (M}^{-1}\text{)}$	n	$\Delta G \text{ (kJ mol}^{-1}\text{)}$
Q	spectrofluorimetry	protonated DNA	7.89 ± 0.20	1.97 ± 0.15	-26.53 ± 1.50
		B DNA	3.67 ± 0.15	3.01 ± 0.20	-25.61 ± 1.45
	Job's method	protonated DNA		1.86 ± 0.14	
		B DNA		2.92 ± 0.25	
M	spectrofluorimetry	protonated DNA	5.29 ± 0.25	2.01 ± 0.15	-25.59 ± 1.60
		B DNA	2.78 ± 0.18	2.93 ± 0.22	-24.93 ± 1.49
	Job's method	protonated DNA		2.22 ± 0.18	
		B DNA		3.03 ± 0.20	

^aAverage of three determinations.

However, the extent of hypochromicity is more in the case of Q (Figure 3B) compared to that of M (Figure 3D). This may be due the presence of a catechol moiety in the B ring of Q which makes Q more reactive. For both cases, the absence of any isosbestic point indicates the nonoccurrence of 1:1 (flavonoid:DNA) stoichiometry and/or there is more than one type of binding. For this reason, absorption data were not used to determine the binding parameters.

Fluorescence Spectral Study. Fluorescence emission spectra of Q and M were monitored in the absence and presence of increasing concentrations of protonated- and B-form DNA (Figure 4). Formation of complex was made by titrating a fixed concentration of the flavonoid and increasing the concentration of both forms of DNA. The effect of protonated DNA with the flavonoid analogs is presented in Figure 4A and 4C. Figure 4 shows a negligible change in the emission intensity of flavonoids upon addition of the protonated form of DNA in the initial stage of interaction. However, on further addition of protonated DNA, significant enhancement in the emission intensity of the analogs was observed associated with the development of a new peak in the region 500–600 nm corresponding to the photoproduct tautomer. This was indicative of strong binding of the flavonoids to protonated DNA, which is due to an effective overlap of the bound flavonoid with the DNA base pairs. This typical behavior clearly indicates that at the initial stage energy transfer from donor to acceptor is not taking place. However, after the addition of a certain concentration of the protonated form of DNA, there is a decrease in either the inter- or the intramolecular distance between the donor and the acceptor which causes a resonance energy transfer (RET) between donor and acceptor. On the other hand, in the case of Q, there was a progressive enhancement in the intensity of the normal form with increasing concentration of B-form DNA along with a decrease in that of the photoproduct tautomer species without any significant shift in λ_{max} (Figure 4B), whereas for M only the emission corresponding to the tautomer species results in buffer 1, and in this case also, intensity decreases with the addition of B-form DNA (Figure 4D). The decrease in fluorescence intensity can also attributed to the micro-environmental change in the flavonoid–B-form DNA system. After a certain concentration of B-form DNA, the emission spectrum of the flavonoids indicates saturation of intensity.

Binding Parameters. Since the evaluation of the binding constant and stoichiometry can give an idea about the mode of binding, we used the emission data by using the following equation⁹

$$\log \frac{F_0 - F}{F} = \log K_a + n \log [P] \quad (4)$$

where F_0 and F are the fluorescence intensities in the absence and presence of DNA, respectively. K_a is the association constant; n indicates the binding stoichiometry of the flavonoid–DNA system, and $[P]$ is the concentration of DNA. The plot of $\log [(F_0 - F)/F]$ vs $\log [P]$ results a straight line. The corresponding binding constant (K_a) and n are determined from the intercept and slope of the aforesaid plot is presented in Table 1. The evaluated binding constant indicates a moderately strong binding of the flavonoid with the protonated form of DNA (K_a for Q and M in the case of protonated DNA is more than double that obtained in the case of B-form DNA–flavonoid complexation). Using the value of K_a , the determined free energy change (ΔG) indicates a favorable complexation process.

Stoichiometry for the Association. The binding stoichiometry of flavonoid–DNA complex was also determined by employing the Job's method (mentioned earlier). The plots for the association of Q and M with the protonated and B form of CT DNA are shown in Figure S2, Supporting Information. From the inflection point, the stoichiometry of binding was calculated, and the data are presented in Table 1. These data agree well with the data obtained from the spectrofluorimetric measurements.

Viscometric Study. In general, intercalation of a ligand between the base pairs of DNA causes enhancement of viscosity of the solution. A higher viscosity of a solution indicates the presence of attractive forces in solution. Therefore, in the case of an intercalator, the attraction between itself and DNA is greater than that of free DNA in solution. This could be attributed to the unwinding of the double helix, which definitely will change the mutual interactions of the molecules. The groove-binding agent, on the other hand, does not cause any disruption of the DNA double helix and hence does not affect the viscosity at all. The effect of change in the specific viscosity of DNA solution in the presence of flavonoid is shown in Figure 5, which indicates that in each case (protonated or B form of DNA) there are negligible changes in viscosity by the addition of flavonoid. The result with the B form is quite reasonable as viscosity does not change in the case of groove binding. However, the probability of intercalation (expected due to the higher binding constant) in the case of the protonated form is also ruled out, as in the case of intercalation viscosity increases significantly. Thus, a high binding constant may be attributed to a strong stacking interaction between the protonated DNA and flavonoids.

CD Studies on the Binding of Q and M to the Protonated and B Form of CT DNA. *Protonated DNA–Flavonoid Interaction.* The CD spectrum of protonated-form DNA was strongly perturbed on interaction with the flavonoids (Figure 6A and 6C). According to Figure 6A, in the case of Q,

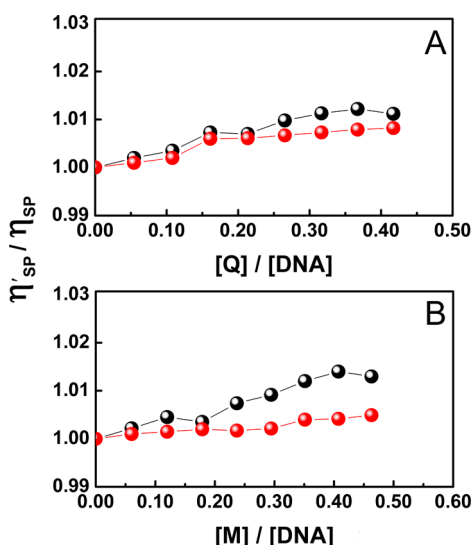


Figure 5. Effect of increasing concentration of Q (A) and M (B) on relative specific viscosity of protonated form (red circles) and B form (black circles) of CT DNA in buffer 1 at 10 °C and buffer 2 at 25 °C. The concentration of CT DNA was 450 μ M.

there was decrease in ellipticity of the broad positive band at \sim 290 nm without any significant shift in wavelength. Another positive band around 260 nm was not modified significantly, and the negative band at \sim 242 nm changed irregularly and ultimately enhanced in ellipticity at saturation. A different behavior was observed in the case of M-protonated DNA interaction (Figure 6C). There was a decrease in ellipticity of the positive band around 290 nm, and it became a sharp band with a \sim 9 nm red shift in wavelength. Enhancement of ellipticity was observed for another positive band around 260

nm and the negative band at 245 nm until saturation, and the negative band was blue shifted. These modifications reflect change of the DNA helix and orientation of the bases to accommodate the flavonoids. Studies on some typical intercalators have shown that enhancement of the CD band at 275 nm of DNA was observed due to drug accommodation into the base pairs.^{27,28} Thus, the binding in both cases may be intercalative or stacking, which causes greater perturbation in the CD spectra of DNA compared to those for typical groove binders. As we have already found from a viscometric study that the binding is not intercalation, there must be a strong stacking interaction between the flavonoids and protonated DNA. Figure 6A and 6C shows that there is an induction of the CD band in the absorption region of Q and M. This is due to the molecular asymmetry induced by the DNA on Q and M. The inset of Figure 6A and 6C represents the induced CD of flavonoids in the presence of DNA. These induced CD spectra appeared in the wavelength region where DNA had no absorption. Thus, the appearance of the CD spectrum was exclusively from the asymmetric arrangement of the flavonoid in the DNA environment. Relatively greater induced CD spectra in the case of Q compared to M also establish the greater asymmetry of Q induced by DNA, which is indicative of a strong stacking interaction.

B Form DNA–Flavonoid Interaction. The effects of the flavonoids Q and M on the CD spectral changes of the B form of CT DNA are depicted in Figure 6B and 6D. The characteristic B-form spectrum of CT DNA was not perturbed significantly in the presence of Q and M, though in the case of Q enhancement in ellipticity of both the positive and the negative band of B-form DNA is observed. No appreciable shift of the bands was noted in the presence of each of the flavonoids. A probable explanation of the change in the 275 nm

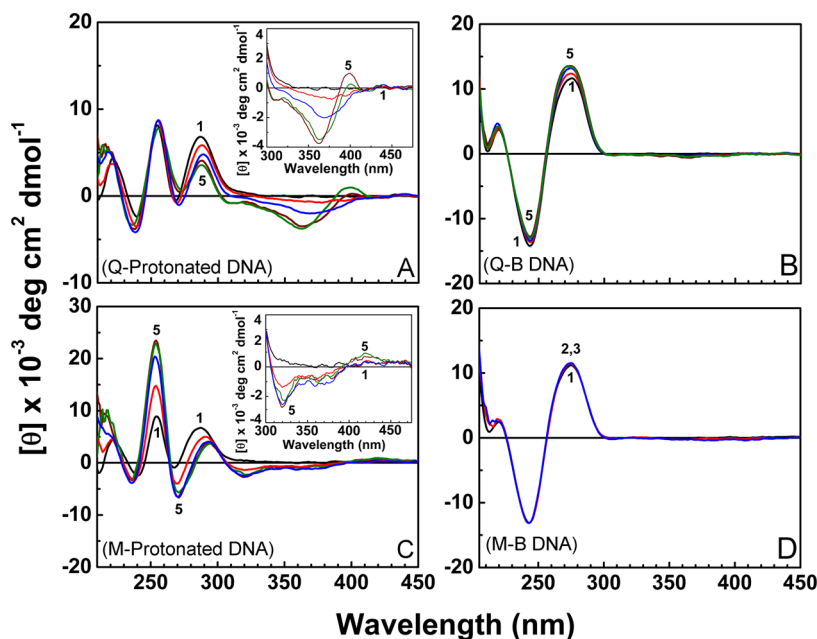


Figure 6. Representative CD spectra for the interaction of Q and M with protonated and B form of CT DNA: (A) Curves 1–5 denote protonated form of CT DNA (100 μ M) treated with 0, 15.45, 32.70, 46.35, and 61.80 μ M Q; (B) Curves 1–5 denote B form of CT DNA (100.0 μ M) treated with 0, 5.15, 10.30, 20.60, and 41.20 μ M Q; (C) Curves 1–5 denote protonated form of CT DNA (100.0 μ M) treated with 0, 14.67, 24.45, 39.12, 58.68, and 78.24 μ M M; (D) Curves 1–3 denote B form of CT DNA (100.0 μ M) treated with 29.34 and 58.68 μ M M. (Inset of A and C) Closest approach on the induced CD spectrum of Q and M, respectively. Titrations with the protonated form of DNA were performed in buffer 1 at 10 °C, and titrations with the B form DNA were carried out in buffer 2 at 25 °C. Expressed molar ellipticity is based on DNA concentration.

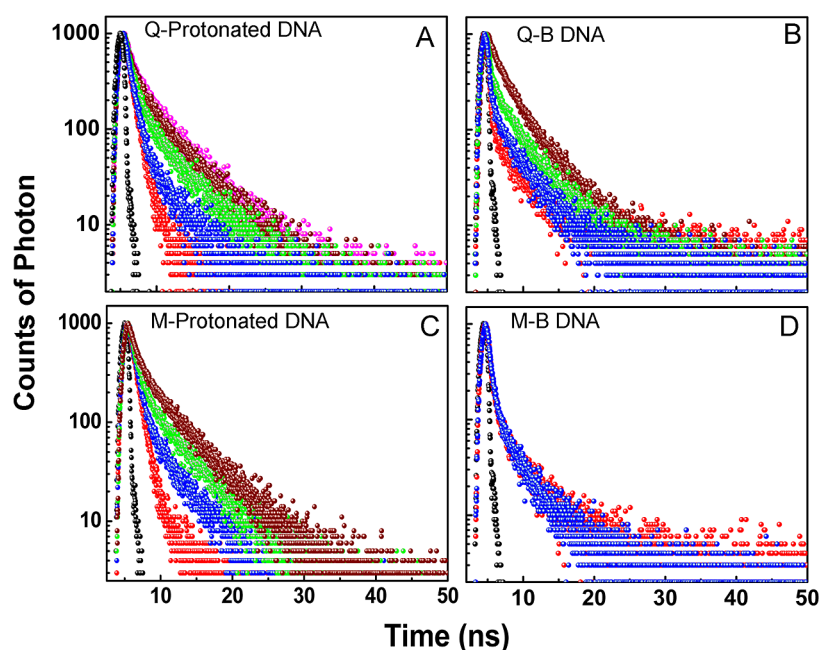


Figure 7. Time-resolved fluorescence decay curves (logarithm of normalized intensity versus time in nanoseconds) for Q and M in the absence and presence of increasing concentration of protonated and B form of CT DNA. (A) Profiles for free 5.15 μM Q (red circles) treated with 12.87 (blue circles), 25.75 (green circles), 38.63 (brown circles), and 51.50 μM (purple circles) and (C) profiles for free 4.89 μM M (red circles) treated with 12.23 (blue circles), 24.45 (green circles), and 48.90 μM (brown circles) protonated form of CT DNA in buffer 1 at 10 $^{\circ}\text{C}$. (B) Profiles for free 5.15 μM Q (red circles) treated with 25.75 (blue circles), 51.50 (green circles), and 103.00 μM (brown circles) and (D) profiles for free 4.89 μM M (red circles) treated with 97.80 μM (blue circles) B form of CT DNA in buffer 2 at 25 $^{\circ}\text{C}$.

Table 2. Lifetime Data for Q and M in the Absence and Presence of the Protonated and B Form of CT DNA in Buffer 1 and Buffer 2^a

flavonoid	[flavonoid] (μM)	DNA	[DNA]/ [flavonoid]	τ_1 (ns)	τ_2 (ns)	CHISQ
Q	5.15	protonated form	0.0	0.89	3.28	1.02 \pm 0.01
			2.5	0.97	4.68	0.98 \pm 0.01
			5.0	1.11	6.27	1.01 \pm 0.02
			7.5	1.23	7.91	0.97 \pm 0.02
			10.0	1.26	7.95	1.01 \pm 0.01
		B form	0.0	0.81	2.97	0.97 \pm 0.04
			5.0	0.85	3.17	1.03 \pm 0.01
			10.0	0.88	3.28	1.04 \pm 0.01
			15.0	0.89	3.37	0.99 \pm 0.02
			20.0	0.91	3.39	1.01 \pm 0.01
M	4.89	protonated form	0.0	0.85	2.97	0.98 \pm 0.03
			2.5	0.96	4.43	1.06 \pm 0.01
			5.0	1.07	5.72	0.99 \pm 0.03
			7.5	1.17	6.72	1.02 \pm 0.02
			10.0	1.19	6.77	1.04 \pm 0.01
		B form	0.0	0.81	2.73	0.98 \pm 0.03
			5.0	0.82	2.75	1.04 \pm 0.01
			10.0	0.82	2.76	1.11 \pm 0.01
			15.0	0.82	2.77	0.99 \pm 0.02
			20.0	0.83	2.77	1.01 \pm 0.01

^aAverage of three determinations.

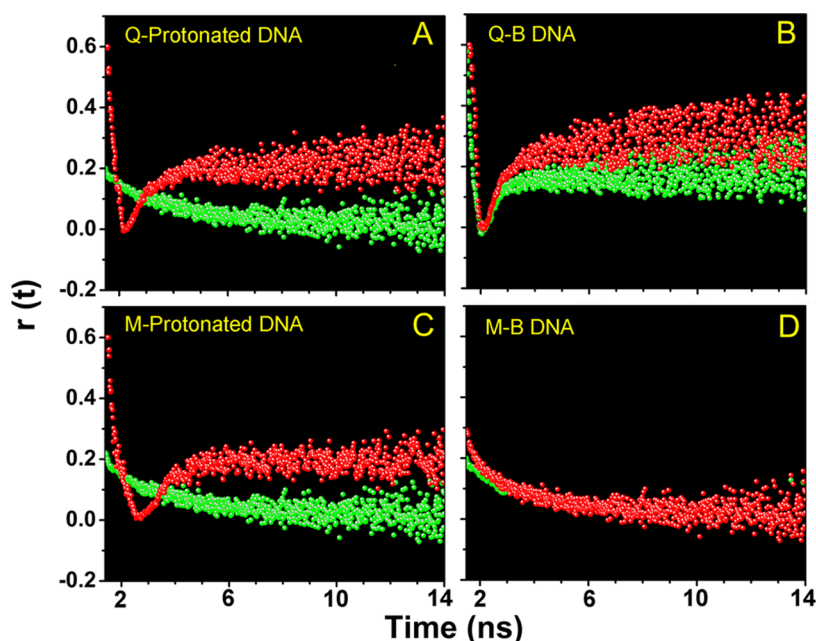
band of B-form DNA is the disruption of stacking of the base pairs. It is observed that the perturbation of the CD spectrum is greater in the presence of Q than that of M. However, the change is relatively less compared to those for typical intercalating agents.^{27,28} Both Q and M are planar and achiral in nature, and thus, they are not CD active. No appearance of induced CD in a wavelength region where DNA has no absorption band clearly indicates that no asymmetry was

induced on the flavonoid in the presence of the B form of DNA.

Lifetime Measurement. Figure 7 represents the TCSPC profiles for Q and M in the absence and presence of both forms of CT DNA. The lifetimes obtained from the best fittings of the decay profiles are presented in Table 2. Biexponential decay was used when a monoexponential decay did not fit well. The results show that both flavonoids have monoexponential decays

Table 3. Parameters Obtained from Steady-State Fluorescence Anisotropy for the Interaction of Q and M with the Protonated and B Form of DNA in Respective Buffers at 10 and 25 °C^a

parameters	methods	environment	values	
			Q	M
$K_a \times 10^{-4}$ (apparent binding constant, M ⁻¹)	spectrofluorimetry	protonated DNA	7.27 ± 0.40	5.74 ± 0.25
		B DNA	3.82 ± 0.45	3.01 ± 0.30
fluorescence polarization anisotropy (r)	spectrofluorimetry	protonated DNA	free: 0.146 ± 0.09	free: 0.081 ± 0.10
			bound: 0.373 ± 0.01	bound: 0.339 ± 0.09
		B DNA	free: 0.150 ± 0.09	free: 0.078 ± 0.08
			bound: 0.270 ± 0.08	bound: 0.182 ± 0.07

^aAverage of three determinations.**Figure 8.** Representative time-resolved fluorescence anisotropy decay profile of Q and M in free and bound state in buffer 1 and buffer 2 at 10 and 25 °C, respectively. (A) Q in free (green circles) and bound condition (red circles) with the protonated form of DNA. (B) Q in free (green circles) and bound condition (red circles) with the B form of DNA. (C) M in free (green circles) and bound condition (red circles) with the protonated form of DNA. (D) M in free (green circles) and bound condition (red circles) with the B form of DNA.

in buffer 1 due to the absence of photoproduct isomer. In both cases the decays are biexponential in nature in the presence of protonated DNA. However, in buffer 2 the decays were biexponential in nature corresponding to the normal and photoproduct isomer, though in the case of M the weight corresponding to the normal isomer is negligible (3.03%) compared to that of the tautomer (96.97%). This again establishes the fact that in pH 7.0, M exclusively exists as an anionic species which was also observed in the characteristic fluorescence spectrum of M (Figure 2). The data presented in Table 2 reveal that in the case of free Q the lifetime was 0.89 and 0.81 ns in buffer 1 and 2, respectively. The lifetime of the first component remains almost constant in the presence of either form of DNA, whereas for the second component the change was 3.28–7.95 ns for protonated DNA and 2.97–3.39 ns for B-form DNA at saturation. From Figure 7D it is clear that the lifetime of M remains unaltered in the presence of B-form DNA, while in the case of protonated DNA the first component remains almost constant as we observed in the case of Q, but the lifetime of the second component changes from 2.97 to 6.77 ns at saturation. Our data clearly conclude that there occurs a partitioning of Q and M in two environments: one is free, and the other is DNA bound. Enhancement in

lifetime values suggests strong binding of the flavonoids to the DNA, and the binding is stronger when the DNA is protonated.

Steady-State and Time-Resolved Fluorescence and Anisotropy Decay Measurements. Steady-state fluorescence anisotropy measurement is an important tool which provides information about the surroundings of a fluorophore. From anisotropy values, we can get an idea about motional restriction on the mobility of the probe in a confined environment. Therefore, it provides clues about the location of the probe within any biological environment.²⁹

Figure S3A and S3B, Supporting Information, represents the variation of steady-state anisotropy (r) of the flavonoids as a function of the DNA concentration. An initial sharp rise in the anisotropy value indicates the enhancement in motional restriction on the flavonoids within DNA environment. There is no significant increase at the later stage, probably due to saturation. Data obtained from steady-state anisotropy are tabulated in Table 3. Data clearly indicate that both Q and M are confined in a motionally restricted region within the DNA environment. The comparatively greater extent of change in the case of protonated DNA indicates greater restriction of motion of the flavonoids in the protonated DNA environment.

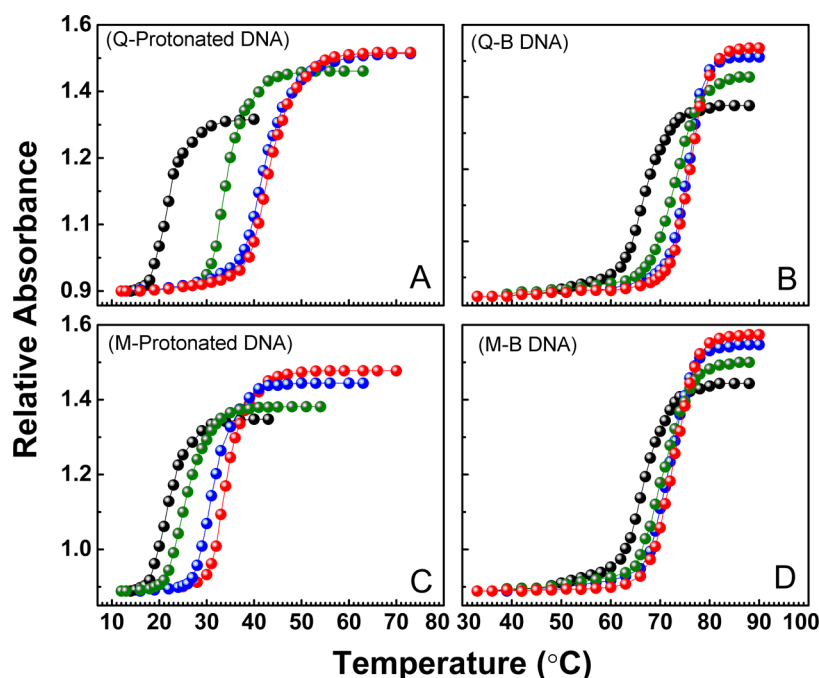


Figure 9. Helix melting profiles of the protonated and B form of CT DNA and their complexation with Q and M: (i) protonated form of CT DNA and its complex with Q (A) and M (C); (ii) B form of CT DNA and its complex with Q (B) and M (D) at D/P = 0.0 (black circles), 0.2 (green circles), 0.4 (blue circles), and 0.6 (red circles).

The steady-state anisotropy measurement has been applied to determine the flavonoid–DNA binding constant according to the method described by Ingersoll and Strollo.³⁰ The binding constant was determined using the following equation

$$\frac{1}{f_B} = 1 + \frac{1}{K_a[P]} \quad (5)$$

Here, K_a is the apparent binding constant, $[P]$ is the concentration of DNA, and f_B is the fractional fluorescence contribution from the DNA-bound flavonoid, and it is defined as follows

$$f_B = \frac{r - r_F}{R(r_B - r) + (r - r_F)} \quad (6)$$

where r_F and r_B are the anisotropy values corresponding to free and DNA-bound flavonoid, respectively. R is the ratio I_B/I_F , which is introduced to ensure the fact that the flavonoid experiences emission intensity modulation upon interaction with DNA. The plot of $1/f_B$ vs $1/[P]$ produces a straight line (not shown) with an intercept of 1 and slope of $1/K_a$. From the slope the calculated values of K_a are presented in Table 3. A commendable agreement with those values obtained from the spectrofluorimetric data thus establishes the reliability and practical applicability of both methods used for evaluation of the binding constant.³¹

To obtain additional information about the surroundings of flavonoids, time-resolved anisotropy decay measurement of Q and M in the buffers and in the DNA environment has been performed. This is a significant tool to investigate the rotational motion and rotational relaxation of the flavonoids trapped within an organized assembly.^{32,33} In a dip and rise profile the dip must be prominent enough to show the exponential rise fairly. In this case the system is getting biased toward an upward curvature at long time (possibly due to a reduced photon count). The fluorescence signal of noise becomes comparable

in the long time regime; as a result, the machine cannot detect the data and noise separately.

Therefore, due to the weak signal-to-noise ratio, scattering occurs. Here, the TCSPC system has somehow become optically nonlinear due to acquisition of data for a single solution over a long period of time. Thus, in the present case we reduced the upper limit of the fitting analysis much below the scattering zone, and after analyzing the data properly we present the time-dependent anisotropy profiles of the free and DNA-bound flavonoids in Figure 8. The flavonoids are seen to exhibit single-exponential anisotropy decay in buffer 1. Interestingly, they are found to demonstrate an unusual “dip-and-rise” pattern in the protonated DNA environment, and the enhancement of the aforesaid pattern is observed with increasing DNA concentration. Such a dip-and-rise pattern is an indication for the appearance of at least two components: one having a shorter fluorescence lifetime and the other with longer lifetime.^{34,35} Such decay profile is best obtained when the two lifetime values are considerably different.^{34–36}

It is understandable that with increasing protonated DNA concentration the population of the photoproduct tautomer of the flavonoids will be progressively encouraged, thereby resulting in the prominent appearance of the dip-and-rise pattern in the anisotropy decay profiles (Figure 8A and 8C). In buffer 2, Q and M show biexponential (so-called dip-and-rise pattern) and single-exponential anisotropy decay, respectively (Figure 8B and 8D). These again established the fact that in buffer 2 Q shows two types of isomers (normal and photoproduct tautomer) and M shows only one type of compound (normal isomer). These data agree well with the data obtained from fluorescence data.

Helix Melting Study of Flavonoid–DNA Complexation. The melting temperature (T_m) is a measure of the thermodynamic stability of the DNA double helix. Stabilization of the protonated and B form DNA was observed in the

presence of Q and M. Stabilization of the double helix is observed when the ligands bind through the mechanism of intercalation or strong stacking, whereas for groove binders a relatively small increase in T_m occurs.^{24,37,38} In this report, we performed the helix melting study of the DNA in free and bound condition, and the results are presented in Figure 9. It has been observed that in the presence of flavonoid at saturation (D/P of 0.6) the extent of stabilization of the protonated form of DNA was ~ 22 and 12.4 °C upon binding to Q and M, respectively. However, at the aforesaid D/P value, less stabilization of the B form of CT DNA was noted (~ 9 °C for Q and ~ 5 °C for M) in the T_m . This data clearly indicates a better stacking of Q with the base pairs compared to that for M. According to Bloomfield et al., the effect of flavonoids on T_m is the result of three reasons:³⁹ (i) the positively charged flavonoid molecules (formed in buffer 1) screen the negatively charged phosphates in the DNA backbone, (ii) enhanced stacking interactions due to the presence of aromatic rings in flavonoids, and (iii) reduction of charge density per unit length along the backbone by locally unwinding the double helix in the presence of the flavonoids. Thus, the observed melting profiles clearly specify a strong stacking interaction of Q and M with the protonated form of DNA. On the other hand, comparatively less stabilization of the B form of DNA in the presence of flavonoids establishes the groove binding between the flavonoids and B-form DNA. A significant increase in T_m of the DNA (as a result of strong stacking or intercalation) or insignificant change in T_m (as a result of groove binding) is reliable with the literature.^{9,24,37–40}

DFT Study: Ground- and Excited-State Geometry Optimization. The optimized normal and tautomer structures of Q and M are shown in Figure S4, Supporting Information. The γ -pyrone ring (ring C) in the case of normal isomer of M is tilted away from the B ring of normal M molecule. The mechanism of electronic excitation of both the ground and the excited states of the flavonoids was studied by exploiting the energy levels of the frontier molecular orbitals, especially the highest occupied molecular orbital (HOMO) and the lowest unoccupied molecular orbital (LUMO). From HOMO–LUMO energy gap we can get an idea about the excited-state intramolecular proton transfer (ESIPT) and hence about the dual-fluorescence behavior of Q and M. The HOMO and LUMO of the respective flavonoids are presented in Figure 10. From the figure it has been observed that in the case of Q the energy of the HOMO of the normal isomer and the LUMO of photoproducted tautomer is quite the same. Hence, for this compound in normal condition (pH 7.0) ESIPT is favorable at the excited state, and as a result a dual-fluorescence behavior of Q is observed. In contrast, in the case of M, the energy gap between the HOMO of normal isomer and the LUMO of tautomer is much higher compared to that of Q. For this compound ESIPT is not favorable. Thus, in either condition (pH 7.0 and 3.4) it exists as a single compound.

Modeling of Flavonoid Binding Site in DNA: Docking Simulation Study. Again, to find out the location of flavonoid molecules in the DNA environment a molecular modeling study has been performed. The details of the method are described in the method section. In recent years, this molecular simulation study has achieved enormous attention and also been described as “very encouraging” by various research groups.^{9,41–43} The docked poses are presented in Figure 11. For both the flavonoids strong external electrostatic interaction is observed (Figure 11A and 11C) when binding is concerned

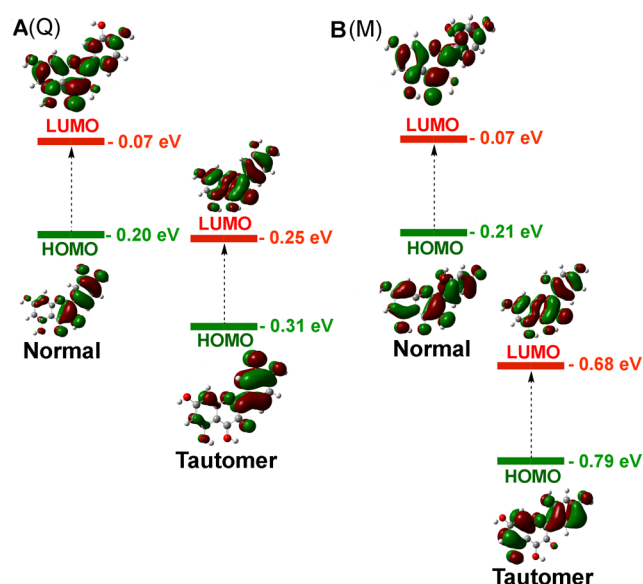


Figure 10. Density plot of the highest occupied molecular orbital (HOMO) and the lowest unoccupied molecular orbital (LUMO) of normal and photoproducted tautomer of Q (A) and M (B) in the excited state.

with the protonated form of DNA. In both cases, hydrogen bonding as well as electrostatic bonding occurs with the phosphate strands and the G–C+ base pair as revealed from the docked pose. Thus, it can be inferred that the appreciable enhancement of the emission spectra of Q and M in the presence of the protonated form of DNA is likely caused by external stacking interactions. Positively charged moieties in a molecule enhance its affinity by interacting with the phosphate backbone of DNA. Thus, these electrostatic interactions are important for achieving high affinity.³¹ In buffer 1, both flavonoids have a positive charge on the γ -pyrone ring, so it is expected that the affinity toward protonated DNA should be high. On the other hand, from Figure 11B and 11D, it is obvious that groove binding of both flavonoids occurs with the B form of DNA, which is quite expected as we observed experimentally. Q binds in the minor groove of B-form DNA, while the major groove of B-form DNA is the encouraging binding site for M. The right panels of each figure mark the DNA bases in the near vicinity (within 4 Å) of the flavonoids. The flavonoid–B-form DNA complex could adjust well into the groove of the DNA with a binding site of three base pairs, preferentially involving the G–C residues. Previously, we used Kaempferol (belongs to the same group of flavonoids like Q and M) to study its interaction with protonated- and B-form DNA, and we found that the results are quite acceptable.⁹

In summary, both Q and M show bathochromic shifts when the pH of the solution is increased, although the shift is more in the case of M. Steady-state fluorescence measurement shows that at pH 3.4 the emission corresponds to the photoproducted tautomer being absent. This is because the protonation of the carbonyl oxygen in ring C ruled out the tautomerization. However, at pH 7.0 the dual fluorescence of Q is observed, whereas M shows only the emission from the tautomer. Spectrophotometric, spectrofluorimetric, fluorescence anisotropy, and circular dichroism study of the interactions of Q and M with CT DNA in vitro suggest the greater affinity of these flavonoids to protonated DNA compared to the B-form DNA. Moreover, in the presence of protonated DNA enhancement in

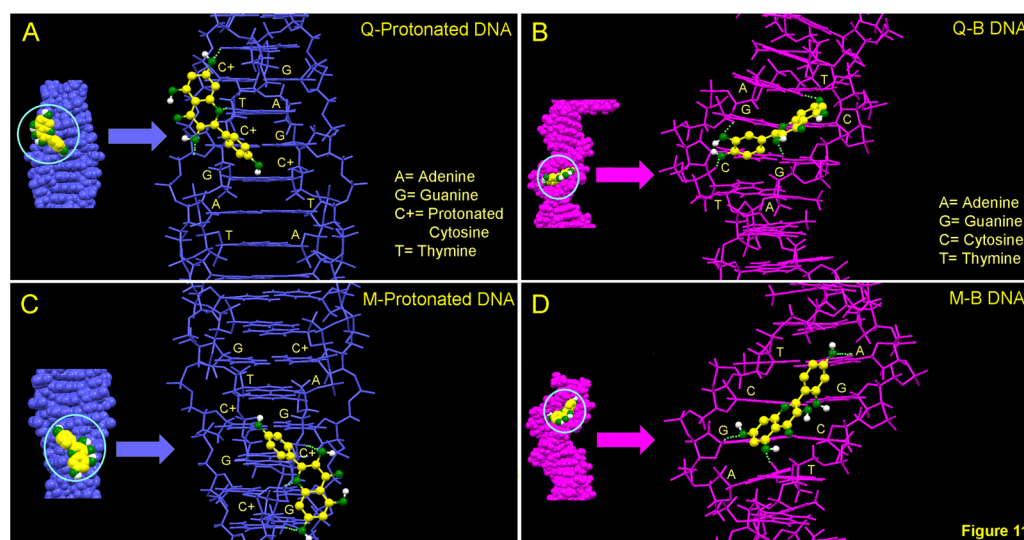


Figure 11. Docked conformation of the flavonoids Q with the (A) protonated form and (B) B form of CT DNA; M with the (C) protonated form and (D) B form of CT DNA. (Right) Near vicinity (within 4.0 Å) of the flavonoid at the interaction site. Dotted line (green) represents the binding of flavonoid molecules with the base pairs.

the tautomer emission results due to ESIPT. Further studies which include fluorescence lifetime measurement and time-resolved fluorescence anisotropy also revealed the presence of both normal and photoproduct tautomer in pH 3.4. Viscosity measurement and a helix melting study revealed that both flavonoids bind to the protonated DNA through electrostatic interaction, whereas groove binding is observed in the B form of DNA. The location of the binding site of the flavonoids was further explained by a molecular docking study.

CONCLUSION

We found that the reactivity of flavonoids is related to the hydroxyl groups present in different positions of the aromatic ring. The presence of hydroxyl groups in the cinnamoyl part affect the reactivity of the flavonoids, and the presence of hydroxyl groups in ring A has no contribution for their reactivity. We used two flavonoids that differ in structure in the position of the hydroxyl groups in ring B. This little difference in structure affects the properties of the flavonoids markedly as we observed from the fluorescence emission spectrum. The acidity of the hydroxyl groups and the HOMO–LUMO energy gap is responsible for the behavior as revealed from DFT study. Moreover, their interaction with the protonated and B form of CT DNA has been studied. From different spectroscopic experiments, viscosity measurement, and molecular docking study it has been found that a strong stacking interaction is responsible for the higher affinity of the flavonoids toward the protonated form of DNA. On the other hand, Q binds to the minor groove and M binds to the major groove of the B form of CT DNA. This array of ionic interactions and groove binding may prove appropriate for selective recognition by small molecules.

ASSOCIATED CONTENT

Supporting Information

Representative absorption spectra, CD spectra, and thermal melting profiles of protonated and B form of CT DNA; representative Job's plot for the association of Q and M with the protonated form and B form of CT DNA; variation of the anisotropy of Q and M fluorescence as a function of

concentration of the protonated form and B form of CT DNA; B3LYP/6-31G-optimized structures of normal and photoproduct tautomer of Q and M. The Supporting Information is available free of charge on the ACS Publications website at DOI: 10.1021/acs.jpcb.5b02827.

AUTHOR INFORMATION

Corresponding Author

*Phone: +91 94 3437 3164, +91033 2457 2349. Fax: +91 33 2414 6266. E-mail: sumandas@chemistry.jdvv.ac.in; sumandas10@yahoo.com.

Notes

The authors declare no competing financial interest.

ACKNOWLEDGMENTS

A.B.P. and L.H. thank the University Grants Commission, Government of India, for the award of a Senior Research Fellowship and Junior Research Fellowship, respectively. S.B. thanks the University Grant Commission, Government of India, for the award of a RGNF research Fellowship. A.G. thanks the Council of Scientific and Industrial Research, Government of India, for the award of a Senior Research Fellowship.

REFERENCES

- (1) Suydam, I. T.; Levandoski, S. D.; Strobel, S. A. Catalytic Importance of a Protonated Adenosine in the Hairpin Ribozyme Active Site. *Biochemistry* **2010**, *49*, 3723–3732.
- (2) Das, S.; Kumar, G. S.; Maiti, M. Conversions of the Left-handed Form and the Protonated Form of DNA Back to the Bound Right-handed Form by Sanguinarine and Ethidium: A Comparative Study. *Biophys. Chem.* **1999**, *76*, 199–218.
- (3) Hoogsteen, K. The Crystal and Molecular Structure of a Hydrogen-Bonded Complex Between 1-Methylthymine and 9-Methyladenine. *Acta Crystallogr.* **1963**, *16*, 907.
- (4) Tajmir-Riahi, H. A.; Neault, J. F.; Naoui, M. Does DNA acid Fixation Produce Left-handed Z Structure? *FEBS Lett.* **1995**, *370*, 105–108.
- (5) Jurasekova, Z.; Domingo, C.; Garcia-Ramos, J. V.; Sanchez-Cortes, S. Effect of pH on the Chemical Modification of Quercetin and Structurally Related Flavonoids Characterized by Optical (UV-visible

- and Raman) Spectroscopy. *Phys. Chem. Chem. Phys.* **2014**, *16*, 12802–12811.
- (6) Roshal, A. D.; Grigorovich, A. V.; Doroshenko, A. O.; Pivovarenko, V. G.; Demchenko, A. P. J. Flavonols as Metal-ion Chelators: Complex Formation with Mg^{2+} and Ba^{2+} Cations in the Excited State. *J. Photochem. Photobiol., A* **1999**, *127*, 89–100.
- (7) Frolov, Y. L.; Sapozhnikov, Y. M.; Brev, S. S.; Pogodaeva, N. N.; Tyukavkina, N. A. *Izv. Akad. Nauk SSSR, Ser. Khim.* **1974**, *10*, 2364–2367.
- (8) Sengupta, P. K.; Kasha, M. Excited State Proton-transfer Spectroscopy of 3-Hydroxyflavone and Quercetin. *Chem. Phys. Lett.* **1979**, *69*, 382–385.
- (9) Pradhan, A. B.; Haque, L.; Bhuiya, S.; Das, S. Exploring the Mode of Binding of the Bioflavonoid Kaempferol with B and Protonated Forms of DNA Using Spectroscopic and Molecular Docking Studies. *RSC Adv.* **2015**, *5*, 10219–10230.
- (10) Gomori, G. Preparation of Buffers for Use in Enzyme Studies. *Methods Enzymol.* **1955**, *1*, 138–146.
- (11) Job, P. Formation and Stability of Inorganic Complexes in Solution. *Ann. Chim. Appl.* **1928**, *9*, 113–203.
- (12) Larsson, A.; Carlsson, C.; Jonsson, M.; Albinsson, B. Characterization of the Binding of the Fluorescent Dyes YO and YOYO to DNA by Polarized Light Spectroscopy. *J. Am. Chem. Soc.* **1994**, *116*, 8459–8465.
- (13) Das, S.; Kumar, G. S. Molecular Aspects on the Interaction of Phenosafranine to Deoxyribonucleic Acid: Model for Intercalative Drug–DNA Binding. *J. Mol. Struct.* **2008**, *872*, 56–63.
- (14) Hay, P. J.; Wadt, W. R. *Ab initio* Effective Core Potentials for Molecular Calculations. Potentials for K to Au Including the Outermost Core Orbitals. *J. Chem. Phys.* **1985**, *82*, 299–310.
- (15) Becke, A. D. Density-functional Thermochemistry. III. The Role of Exact Exchange. *J. Chem. Phys.* **1993**, *98*, 5648–5652.
- (16) Barone, V.; Cossi, M.; Tomasi, J. Geometry Optimization of Molecular Structures in Solution by the Polarizable Continuum Model. *J. Comput. Chem.* **1998**, *19*, 404–417.
- (17) Bhadra, K.; Kumar, G. S.; Das, S.; Islam, M.; Maiti, M. Protonated Structures of Naturally Occurring Deoxyribonucleic Acids and their Interaction with Berberine. *Bioorg. Med. Chem.* **2005**, *13*, 4851–4863.
- (18) Kumar, G. S.; Das, S.; Bhadra, K.; Maiti, M. Protonated Forms of Poly[d(G-C)] and Poly(dG).poly(dC) and Their Interaction with Berberine. *Bioorg. Med. Chem.* **2003**, *11*, 4861–4870.
- (19) Zsila, F.; Bikadi, Z.; Simonyi, M. Probing the Binding of the Flavonoid, Quercetin to Human Serum Albumin by Circular Dichroism, Electronic Absorption Spectroscopy and Molecular Modelling Methods. *Biochem. Pharmacol.* **2003**, *65*, 447–456.
- (20) Huang, L.; Yu, D. Q. *The Application of Ultra-Violet Spectroscopy in Organic Chemistry*; Scientific Press: Beijing, 1988.
- (21) Tommasini, S.; Calabro, M. L.; Donato, P. Improvement of Solubility and Dissolution Rate of Complexes of Flavonoids with β -Cyclodextrin and their Thermodynamic Properties. *J. Pharm. Biomed. Anal.* **2004**, *35*, 389–397.
- (22) Jovanovic, S. V.; Steeden, S.; Tosic, M.; Marjanovic, B.; Simic, M. G. Flavonoids as Antioxidants. *J. Am. Chem. Soc.* **1994**, *116*, 4846–4850.
- (23) Chaudhuri, S.; Basu, K.; Sengupta, B.; Banerjee, A.; Sengupta, P. K. Ground- and Excited-state Proton Transfer and Antioxidant Activity of 3-Hydroxyflavone in Egg Yolk Phosphatidylcholine Liposomes: Absorption and Fluorescence Spectroscopic Studies. *Luminescence* **2008**, *23*, 397–403.
- (24) Jana, B.; Senapati, S.; Ghosh, D.; Bose, D.; Chattopadhyay, N. Spectroscopic Exploration of Mode of Binding of ctDNA with 3-Hydroxyflavone: A Contrast to the Mode of Binding with Flavonoids Having Additional Hydroxyl Groups. *J. Phys. Chem. B* **2012**, *116*, 639–645.
- (25) Long, E. C.; Barton, J. K. On Demonstrating DNA Intercalation. *Acc. Chem. Res.* **1990**, *3*, 271–273.
- (26) Tysoe, S. A.; Morgan, R. J.; Baker, A. D.; Streckas, T. C. Spectroscopic Investigation of Differential Binding Modes of DELTA- and LAMBDA-Ru(bpy)₂(ppz)²⁺ with Calf Thymus DNA. *J. Phys. Chem.* **1993**, *97*, 1707–1711.
- (27) Dalglish, D. G.; Peacocke, A. R.; Fey, G.; Harvey, C. The Circular Dichroism in the Ultraviolet of Aminoacridines and Ethidium Bromide Bound to DNA. *Biopolymers* **1971**, *10*, 1853–1863.
- (28) Palumbo, M.; Capasso, L.; Palu, G.; Marcianimagno, S. Conformational Aspects of Drug–DNA Interactions: Studies on Anthracycline Antibiotics and Psoralen Derivatives. *Proc. Int. Symp. Biomol. Struct. Interact., Suppl. J. Biosci.* **1985**, *8*, 689–697.
- (29) Lakowicz, J. R. *Principles of Fluorescence Spectroscopy*; Plenum Press: New York, 2006.
- (30) Ingersoll, C. M.; Strollo, C. M. Steady State Fluorescence Anisotropy to Investigate Flavonoids Binding to Proteins. *J. Chem. Educ.* **2007**, *84*, 1313–1315.
- (31) Ganguly, A.; Paul, B. K.; Ghosh, S.; Dalapati, S.; Guchhait, N. Interaction of a Potential Chloride Channel Blocker with a Model Transport Protein: a Spectroscopic and Molecular Docking Investigation. *Phys. Chem. Chem. Phys.* **2014**, *16*, 8465–8475.
- (32) Paul, B. K.; Samanta, A.; Guchhait, N. Exploring Hydrophobic Subdomain IIA of the Protein Bovine Serum Albumin in the Native, Intermediate, Unfolded, and Refolded States by a Small Fluorescence Molecular Reporter. *J. Phys. Chem. B* **2010**, *114*, 6183–6196.
- (33) Paul, B. K.; Guchhait, N. Modulation of Prototropic Activity and Rotational Relaxation Dynamics of a Cationic Biological Photosensitizer within the Motionally Constrained Bio-environment of a Protein. *J. Phys. Chem. B* **2011**, *115*, 10322–10334.
- (34) Bhattacharya, B.; Nakka, S.; Guruprasad, L.; Samanta, A. Interaction of Bovine Serum Albumin with Dipolar Molecules: Fluorescence and Molecular Docking Studies. *J. Phys. Chem. B* **2009**, *113*, 2143–2150.
- (35) Banerjee, D.; Srivastava, S. K.; Pal, S. K. Spectroscopic Studies on Ligand–Enzyme Interactions: Complexation of α -Chymotrypsin with 4',6-Diamidino-2-phenylindole (DAPI). *J. Phys. Chem. B* **2008**, *112*, 1828–1833.
- (36) Ludescher, R. D.; Peting, L.; Hudson, S.; Hudson, B. Time-resolved Fluorescence Anisotropy for Systems with Lifetime and Dynamic Heterogeneity. *Biophys. Chem.* **1987**, *28*, 59–75.
- (37) Kumar, C. V.; Turner, R. S.; Asuncion, E. H. Groove Binding of a Styrylcyanine Dye to the DNA Double Helix: the Salt Effect. *J. Photochem. Photobiol., A* **1993**, *74*, 231–238.
- (38) Paul, B. K.; Guchhait, N. Exploring the Strength, Mode, Dynamics, and Kinetics of Binding Interaction of a Cationic Biological Photosensitizer with DNA: Implication on Dissociation of the DrugDNA Complex via Detergent Sequestration. *J. Phys. Chem. B* **2011**, *115*, 11938–11949.
- (39) Bloomfield, V. A.; Crothers, D. M.; Tinoco, J. I. *Nucleic Acids Structures, Properties and Functions*; University Science Books: Sausalito, CA, 2000.
- (40) David-Cordonnier, M. H.; Laine, W.; Lansiaux, A.; Rosu, F.; Colson, P.; de Pauw, E.; Michel, S.; Tillequin, F.; Koch, M.; Hickman, J. A.; et al. Covalent Binding of Antitumor Benzoacronycines to Double-stranded DNA Induces Helix Opening and the Formation of Single-stranded DNA: Unique Consequences of a Novel DNA-Bonding Mechanism. *Mol. Cancer Ther.* **2005**, *4*, 71–80.
- (41) Campbell, S. J.; Gold, N. D.; Jackson, R. M.; Westhead, D. R. Ligand Binding: Functional Site Location, Similarity and Docking. *Curr. Opin. Struct. Biol.* **2003**, *13*, 389–395.
- (42) Monti, S.; Manet, I.; Manoli, F.; Marconi, G. Structure and Properties of Licochalcone A–Human Serum Albumin Complexes in Solution: a Spectroscopic, Photophysical and Computational Approach to Understand Drug–protein Interaction. *Phys. Chem. Chem. Phys.* **2008**, *10*, 6597–6606.
- (43) Thomas, J. R.; Hergenrother, P. J. Targeting RNA with Small Molecules. *Chem. Rev.* **2008**, *108*, 1171–122.